

Measure an array of cytokines in COVID-19 samples with our multiplex flow cytometry assays.

Read our app note ►



## Cross-Species Transcriptional Network Analysis Defines Shared Inflammatory Responses in Murine and Human Lupus Nephritis

This information is current as of February 26, 2022.

Celine C. Berthier, Ramalingam Bethunaickan, Tania Gonzalez-Rivera, Viji Nair, Meera Ramanujam, Weijia Zhang, Erwin P. Bottinger, Stephan Segerer, Maja Lindenmeyer, Clemens D. Cohen, Anne Davidson and Matthias Kretzler

*J Immunol* 2012; 189:988-1001; Prepublished online 20 June 2012;

doi: 10.4049/jimmunol.1103031

<http://www.jimmunol.org/content/189/2/988>

### Supplementary Material

<http://www.jimmunol.org/content/suppl/2012/06/20/jimmunol.1103031.DC1>

### References

This article **cites 60 articles**, 24 of which you can access for free at: <http://www.jimmunol.org/content/189/2/988.full#ref-list-1>

Why *The JI*? [Submit online.](#)

- **Rapid Reviews! 30 days\*** from submission to initial decision
- **No Triage!** Every submission reviewed by practicing scientists
- **Fast Publication!** 4 weeks from acceptance to publication

*\*average*

### Subscription

Information about subscribing to *The Journal of Immunology* is online at: <http://jimmunol.org/subscription>

### Permissions

Submit copyright permission requests at: <http://www.aai.org/About/Publications/JI/copyright.html>

### Email Alerts

Receive free email-alerts when new articles cite this article. Sign up at: <http://jimmunol.org/alerts>



# Cross-Species Transcriptional Network Analysis Defines Shared Inflammatory Responses in Murine and Human Lupus Nephritis

Celine C. Berthier,<sup>\*,1</sup> Ramalingam Bethunaickan,<sup>†,1</sup> Tania Gonzalez-Rivera,<sup>‡,1</sup> Viji Nair,<sup>\*</sup> Meera Ramanujam,<sup>†</sup> Weijia Zhang,<sup>§</sup> Erwin P. Bottinger,<sup>§</sup> Stephan Segerer,<sup>¶</sup> Maja Lindenmeyer,<sup>¶</sup> Clemens D. Cohen,<sup>¶</sup> Anne Davidson,<sup>†</sup> and Matthias Kretzler<sup>\*</sup>

Lupus nephritis (LN) is a serious manifestation of systemic lupus erythematosus. Therapeutic studies in mouse LN models do not always predict outcomes of human therapeutic trials, raising concerns about the human relevance of these preclinical models. In this study, we used an unbiased transcriptional network approach to define, in molecular terms, similarities and differences among three lupus models and human LN. Genome-wide gene-expression networks were generated using natural language processing and automated promoter analysis and compared across species via suboptimal graph matching. The three murine models and human LN share both common and unique features. The 20 commonly shared network nodes reflect the key pathologic processes of immune cell infiltration/activation, endothelial cell activation/injury, and tissue remodeling/fibrosis, with macrophage/dendritic cell activation as a dominant cross-species shared transcriptional pathway. The unique nodes reflect differences in numbers and types of infiltrating cells and degree of remodeling among the three mouse strains. To define mononuclear phagocyte-derived pathways in human LN, gene sets activated in isolated NZB/W renal mononuclear cells were compared with human LN kidney profiles. A tissue compartment-specific macrophage-activation pattern was seen, with NF- $\kappa$ B1 and PPAR $\gamma$  as major regulatory nodes in the tubulointerstitial and glomerular networks, respectively. Our study defines which pathologic processes in murine models of LN recapitulate the key transcriptional processes active in human LN and suggests that there are functional differences between mononuclear phagocytes infiltrating different renal microenvironments. *The Journal of Immunology*, 2012, 189: 988–1001.

Systemic lupus erythematosus (SLE) is an autoimmune disorder characterized by loss of tolerance to nucleic acids and their binding proteins, resulting in the production of autoantibodies that initiate inflammation or injury. Lupus nephritis (LN) is a major cause of end-organ damage in SLE and is a risk factor for mortality (1, 2). Despite many advances in the diagnosis and management of LN, the incidence of end-stage renal disease secondary to SLE has not decreased in the last 20 y (3, 4). The complex and heterogeneous nature of SLE has represented a challenge for defining pathogenesis and developing effective therapeutics.

Murine models that spontaneously develop lupus (5, 6) have played a key role in our understanding of human disease (7) and have been used extensively for the identification of therapeutic targets. However, there are fundamental differences in the genetic composition of mice and humans that extend to both the innate

and the adaptive immune systems (8, 9); disappointingly, translating the therapeutic successes in animal models to successful clinical interventions for nephritis has been challenging. Therefore, there is a pressing need for a scientific approach that allows the exploration of the similarities and differences among species.

To define shared pathogenetic mechanisms in the development of LN in mice and humans and to determine which mouse model most accurately reflects specific molecular pathways occurring in human disease, we compared gene-expression profiles from microdissected human LN kidney biopsies and whole kidneys from three SLE-prone murine models: NZB/W, NZM2410, and NZW/BXSB. The NZB/W female mouse (10) is characterized by hypercellular renal lesions and fibrinoid necrosis, similar to the lesions seen in class IV human LN kidney specimens (11). NZM2410 mice are characterized by high levels of IL-4 and the production of autoantibodies of the IgG1 and IgE isotypes; they develop a rapidly

<sup>\*</sup>Division of Nephrology, Department of Internal Medicine, University of Michigan, Ann Arbor, MI 48109; <sup>†</sup>Center for Autoimmunity and Musculoskeletal Diseases, Feinstein Institute for Medical Research, Manhasset, NY 11030; <sup>‡</sup>Division of Rheumatology, Department of Internal Medicine, University of Michigan, Ann Arbor, MI 48109; <sup>§</sup>Department of Medicine, Mount Sinai School of Medicine, New York, NY 10029; and <sup>¶</sup>Division of Nephrology, University Hospital Zurich, Zurich, 8091 Switzerland

<sup>1</sup>C.C.B., R.B., and T.G.-R. contributed equally to this work and share first authorship.

Received for publication October 24, 2011. Accepted for publication May 14, 2012.

This work was supported by National Institutes of Health Grants R01 DK085241 (to A.D.) and R01 DK079912 and P30 DK081943 (to M.K.) and by the Alliance for Lupus Research (to A.D. and M.K.). C.C.B. was supported by research fellowship FLB1245 from the National Kidney Foundation. R.B. was supported by a Kirkland Scholar Award (Rheumatism). S.S. is supported by a grant from the University of Zurich, a Clinical Evidence Council grant from Baxter Healthcare Corporation, and a grant from the Swiss National Science Foundation (SNF 32003B\_129710).

The microarray data presented in this article have been submitted to Gene Expression Omnibus (<http://www.ncbi.nlm.nih.gov/geo/>) under accession numbers GSE27045, GSE32583, GSE32591, GSE35488, and GSE37463.

Address correspondence and reprint requests to Dr. Matthias Kretzler or Dr. Anne Davidson, Division of Nephrology, Department of Internal Medicine, University of Michigan, 1150 W. Medical Center Drive, 1570A MSRB II, Ann Arbor, MI 48109 (M.K.) or Feinstein Institute for Medical Research, 350 Community Drive, Manhasset, NY 11030 (A.D.). E-mail addresses: kretzler@umich.edu (M.K.) and adavidson1@nshs.edu (A.D.)

The online version of this article contains supplemental material.

Abbreviations used in this article: DC, dendritic cell; DC-SIGN, dendritic cell-specific intercellular adhesion molecule-3-grabbing nonintegrin; ERCB, European Renal cDNA Bank; GEO, Gene Expression Omnibus; HT, hypertensive nephropathy; IgAN, IgA nephropathy; LD, living donor; LN, lupus nephritis; SLE, systemic lupus erythematosus; TALE, Tool for Approximate LargeE graph matching.

Copyright © 2012 by The American Association of Immunologists, Inc. 0022-1767/12/\$16.00

progressive glomerulosclerosis with scant lymphocytic infiltrate in the kidneys (12). Males of the NZW/BXSB strain carry the *Yaa* (Y-linked autoimmune acceleration) locus that contains a reduplication of the *Tlr7* gene (13). These mice develop an acute proliferative glomerulonephritis with severe tubulointerstitial inflammation (14). The three strains have different autoantibody profiles, with the production of anti-dsDNA Abs in the NZB/W mouse, anti-nucleosome Abs in the NZM2410 mouse, and anti-Sm Ag/ribonucleoprotein and anti-phospholipid Abs in the NZW/BXSB mouse. They also respond differently to therapeutic intervention (15); this underscores the effect of genetic heterogeneity not only on disease phenotype but also on responses to therapies. Analysis of comprehensive renal-expression profiles with unbiased natural language-processing tools (Genomatrix BiblioSphere) and a suboptimal matching algorithm based-approach (Tool for Approximate LargeE graph matching [TALE]) identified multiple shared key conserved regulatory network hubs (nodes) among the three mouse strains and the human LN samples. These pathway maps allow selection of the mouse model with the highest degree of similarity to the human disease or with activation of a pathway of interest for further therapeutic interventions or mechanistic studies in the model system. We found that the sclerotic kidneys of the NZM2410 mice shared the most renal transcriptional events with human LN kidneys, followed by the NZB/W and the NZW/BXSB mice.

We previously showed that the onset of proteinuria in all three strains of mice is associated with the expansion and activation of a dominant population of resident renal mononuclear phagocytes that have a resting phenotype of CD11b<sup>+</sup>/CD11c<sup>int</sup>/F4/80<sup>hi</sup>/Gr1<sup>lo</sup>/MHC<sup>hi</sup> and have variably been referred to as intrinsic renal macrophages or resident renal dendritic cells (DCs), because of their mixed function as both APCs and phagocytic cells (16). At nephritis onset, these cells markedly upregulate their expression of CD11b, and they accumulate both in the interstitium and in the periglomerular space (14, 17, 18). In NZB/W mice, we demonstrated a marked change in the gene-expression profile of isolated F4/80<sup>hi</sup> renal macrophages at proteinuria onset, with the expression of proinflammatory, anti-inflammatory, and tissue repair genes (17). We show in this article that this macrophage profile is shared by the human LN samples but that there are significant differences in the gene-expression profiles of the glomerular and interstitial compartments, suggesting functional differences in this cell type in the two intrarenal microenvironments.

## Materials and Methods

### NZW/W, NZM2410, and NZW/BXSB SLE mouse strains

NZW/W F1 mice were purchased from The Jackson Laboratory (Bar Harbor, ME), NZM2410 mice were purchased from Taconic (Hudson, NY), and NZW/BXSB F1 male mice were bred in our facility from the respective parents (The Jackson Laboratory). All mice were housed in a specific pathogen-free facility with 12-h light/dark cycles and unlimited access to food and water. All animal experiments were approved by the Institute Animal Care and Use Committee of the Feinstein Institute. Supplemental Table I provides details of the subgroups of mice analyzed from each mouse strain, as described in previous publications (14, 18, 19). Briefly, the NZB/W F1 strain included groups of the following ages: 16 wk old (control group without any serum autoantibodies, immune complex deposition, or proteinuria,  $n = 8$ ), 23 wk old (prenephritic control group, with serum autoantibodies, minimal immune complex deposition, and proteinuria  $< 100$  mg/dl,  $n = 11$ ), 23 wk old (with abundant immune complex deposition and new onset of proteinuria  $> 300$  mg/dl,  $n = 6$ ), and 36 wk old (with established proteinuria  $> 300$  mg/dl for  $> 2$  wk,  $n = 10$ ) (20).

NZM2410 mice were 7 wk old (control group without autoantibodies, renal immune complex deposition, or proteinuria,  $n = 5$ ) and 22–30 wk old (with proteinuria  $> 300$  mg/dl for 7–10 d,  $n = 5$ ) (18). Mice of this strain were harvested 7–10 d after proteinuria onset, because most NZM2410 mice die within 14 d of proteinuria onset.

NZW/BXSB mice (14) were 8 wk old (control group, without serum autoantibodies or proteinuria  $n = 4$ ), 17 wk old (prenephritic control group, with serum autoantibodies, proteinuria  $\leq 100$  mg/dl, and histologic glomerular score  $\leq 2$ ,  $n = 6$ ), and 18–21 wk old (with  $> 7$ -d proteinuria  $> 300$  mg/dl and histologic glomerular score  $> 2$ ,  $n = 6$ ).

### Human renal biopsy samples

Human renal biopsies were collected after informed consent was obtained, according to the guidelines of the respective local ethics committees. A total of 47 samples from the European Renal cDNA Bank (ERCB) (21) was processed and used for microarray analysis: pretransplant healthy living donors (LDs) ( $n = 15$ ) and LN patients ( $n = 32$ ). For real-time PCR, 11 LD and 9 LN samples were used from an independent cohort (of the ERCB). Demographic, clinical, and histologic characteristics of these patients are provided in Supplemental Table I. There was no statistical difference in any parameters between the LN cohorts used in arrays and RT-PCR.

### Murine and human RNA extraction, microarray preparation, and processing

Kidneys were removed from perfused mice and immediately snap frozen. Tissues were homogenized in 3 ml TRIzol reagent, and RNA was isolated according to the manufacturer's instructions. cDNA was generated from 5  $\mu$ g total RNA and labeled with biotin using the Ovation Biotin system (NuGEN Technologies, San Carlos, CA). Biotin-labeled cDNA was fragmented and hybridized to Affymetrix Mouse Genome 430 2.0 GeneChip arrays (Santa Clara, CA). After hybridization, GeneChip arrays were washed, stained, and scanned with a GeneChip Scanner 3000 7G, according to the Affymetrix Expression Analysis Technical Manual ([http://media.affymetrix.com/support/downloads/manuals/expression\\_analysis\\_technical\\_manual.pdf](http://media.affymetrix.com/support/downloads/manuals/expression_analysis_technical_manual.pdf)). CD11b<sup>hi</sup>/CD11c<sup>int</sup>/F4/80<sup>hi</sup> mononuclear cells from perfused NZB/W mouse kidneys were isolated by fluorescence cell sorting, as previously described (17), using Abs to CD11b, CD11c, and F4/80. RNA was extracted, amplified, and analyzed using gene-expression profiling, as previously described (17). Normalized data are available at the Gene Expression Omnibus (GEO) Web site (<http://www.ncbi.nlm.nih.gov/geo/>) under accession number GSE27045.

Cortical tissue segments from human biopsy samples were manually microdissected into glomerular and tubulointerstitial compartments, as previously described (22–24). Total RNA was isolated from the microdissected human tissues using the RNeasy mini kit (QIAGEN), according to the manufacturer's instructions. Gene-expression profiling from microdissected human kidney biopsies was performed, as previously described, using the Human Genome U133A Affymetrix GeneChip arrays (Santa Clara, CA) (22, 23).

### Murine and human gene-expression data processing and analysis

The mouse and human CEL files were processed using the GenePattern analysis pipeline (<http://www.genepattern.com>). CEL file normalization was performed with the Robust Multichip Average method using the mouse and human Entrez-Gene custom CDF annotation from Brain Array version 10 (<http://brainarray.mbni.med.umich.edu/Brainarray/default.asp>). The normalized files were log<sub>2</sub> transformed, and batch correction was performed for the NZB/W and NZW/BXSB murine data (25).

The Poly-A RNA Control Kit was used for processing the mouse microarray data. The expression baseline was defined by calculating the gene-expression median of each gene and adding 1 SD to the minimum value obtained. Of the 16,539 mouse genes represented on the Affymetrix GeneChip, 13,425, 13,600, and 14,252 were expressed above the defined expression baseline in NZB/W, NZM2410, and NZW/BXSB mice, respectively. Of the 12,029 human genes, 11,285 and 11,429 were expressed above the 27 Poly-A Affymetrix control expression baseline (negative controls) in the glomerular and tubulointerstitial compartments, respectively, and were used for further analyses. Mouse and human normalized data files were uploaded to the GEO Web site (<http://www.ncbi.nlm.nih.gov/geo/>) under accession numbers GSE32583 and GSE32591.

IgA nephropathy (IgAN) and hypertensive nephropathy (HT) gene-expression profiles from ERCB cohorts were available to the investigators as part of an independent study (W. Ju, C.S. Greene, F. Eichinger, V. Nair, J.F. Hodgins, M. Bitzer, Y.S. Lee, Q. Zhu, M. Kehata, M. Li, et al., submitted for publication) and were compared with the presented LN data. IgAN and HT data will be available on the GEO Web site upon acceptance of the W. Ju et al. manuscript under accession numbers GSE35488 and GSE37463.

### Real-time PCR analysis of human samples

RT and real-time PCR were performed, as reported previously (22). Pre-developed TaqMan reagents (ABI Assays-on-demand) were used for all



genes analyzed. The expression of each gene was normalized to the geometric mean of the housekeeping genes 18S rRNA, PGK1, and GAPDH (26). Those three reference genes were selected as described (27), as well as based on their low variance and absence of regulation in LN compared with LD in arrays. mRNA expression was analyzed by the  $\Delta\Delta$ -Ct method, following the manufacturer's instructions (User Bulletin #2, ABI Prism 7700 Sequence Detection System).

### Cross-species comparison

To avoid ambiguity, the mouse genes were converted to the corresponding human orthologs using the National Center for Integrative Biomedical Informatics homolog (Build 64) and Genomatix annotated ortholog databases. Differential gene expression was defined by a  $q$  value  $< 0.05$ , with a fold change  $\geq 1.2$  for the upregulated genes and  $\leq 0.8$  for the down-regulated genes.

### Network and pathway analyses

Significantly regulated genes were analyzed by creating biological literature-based networks using Genomatix BiblioSphere software (<http://www.genomatix.de>). Canonical pathways were extracted using Ingenuity Pathway Analysis software (<http://www.ingenuity.com>).

### TALE analysis

TALE was used to compare the resulting large transcriptional networks from humans and mice (see Ref. 28 for technical implementation). This algorithm allows comparison of large networks (often with 1000s of nodes and edges) and extraction of meaningful relationships between the query and database networks. TALE allows definition of the degree of mismatch tolerance in the resulting overlapping network. In addition to the query network and the database networks, TALE requires three fields of user inputs: a similarity assignment for the genes in the networks, the percentage of important nodes, and the percentage of mismatch. The first parameter is required to group the nodes in the networks. For cross-species comparison, the orthologous information was used to group the human and mouse genes. The second parameter defines the set of seed genes in the query network to generate the overlapping network. In this setting, the importance of a node (or a gene) is defined by the number of connections that it has with the remaining genes in the human network. In the current study, the top 10% of nodes was used to build the core network elements. The third parameter defines the mismatch allowed while generating the neighborhood of the seed genes, as well as extending the network; a mismatch tolerance of 10% was set in the current study. The transcriptional networks (human and mice) generated from the literature-based Genomatix BiblioSphere software (gene/function word/gene [B3] filter) were used as input. The resulting mouse networks were populated into the database, and the human network was used as the query network. The resulting TALE networks were visualized using Cytoscape version 2.7 (29).

Prior to the comparison of each murine model with human LN, a preliminary TALE analysis was performed within the NZB/W and NZW/BXSB models to define which group comparison (corresponding to different disease stages, Table I) most closely resembled the human data sets. The NZB/W analysis included the following comparisons: 36-wk old with established nephritis compared with 16- or 23-wk-old prenephritic, as well as 23-wk old at onset of proteinuria compared with 16- or 23-wk-old prenephritic. The 36-wk-old mice with established proteinuria, compared with the 23-wk-old prenephritic mice, shared the highest number of transcriptional network nodes with the human tubulointerstitium LN versus control tubulointerstitium; in comparison with the human glomerular LN dataset, the 36- versus 16-wk-old mice had the greatest overlap. These datasets were subsequently used for further analysis. Similarly, we compared the results for either 8- or 17-wk prenephritic NZW/BXSB with 18–21-wk nephritic NZW/BXSB mice and found that they were similar (Table I). Therefore, we used the larger 17-wk prenephritic control group for the comparison analyses.

### Immunohistochemistry

To localize macrophages and DCs in human LN, archival sections from 10 renal biopsies with LN class IV (International Society of Nephrology/Renal Pathology Society 2003 classification) and 5 preimplantation biopsies were studied. Immunohistochemistry was performed, as previously described (30). The monoclonal mouse anti-CD68 (clone PG-M1; Dako, Germany, Hamburg), mouse anti-DC-specific intercellular adhesion molecule-3-grabbing nonintegrin SIGN (DC-SIGN; CD209, clone DCN46; BD Pharmingen, Heidelberg, Germany), and polyclonal rabbit anti-S100 (Dako) were used.

### Statistical analysis

For the array study, statistical unpaired analyses for each comparison between the relevant study groups were performed using the Significance Analysis of Microarrays method implemented in the MultiExperiment Viewer application (31, 32). Genes regulated between two groups with a  $q$ -value (false discovery rate)  $< 0.05$  were considered significant and used for further transcriptional and pathway analyses. A Student  $t$  test was used for the RT-PCR study; a  $p$  value  $< 0.05$  was considered significant.

## Results

### Renal LN cross-species functional analysis

Differentially regulated genes were identified from the kidneys of mice with LN compared with prediseased controls and from humans with LN compared with healthy kidneys. Human LN kidneys demonstrated 3159 glomerular and 2261 tubulointerstitial genes with mRNA expression significantly modified compared with LD kidneys. Lupus mice were compared with their prenephritic counterparts, using the same significance criteria and fold change as in the human study. A total of 2642, 4015, and 2900 genes was differentially regulated in NZB/W mice (36-wk old with established proteinuria compared with 23-wk-old prenephritic), NZM2410 mice (22–30-wk nephritic compared with 7-wk prenephritic controls), and NZW/BXSB mice (18–21-wk nephritic compared with 17-wk prenephritic), respectively. Real-time PCR validation of 120 genes confirmed  $>85\%$  of the genes identified in the microarray analysis (R. Bethunaickan, C. Berthier, M. Kretzler, and A. Davidson, manuscript in preparation). Table I displays the number of genes significantly regulated in the murine disease groups available for analyses, as well as the number of regulated genes overlapping with the human data in each renal compartment. Murine data sets with the highest degree of overlap in the network-level comparison were used for further studies (see *Materials and Methods* for more details) (Table I).

Gene-expression profiles from whole mouse kidneys were compared with profiles from human microdissected kidneys. This study compares the murine whole-kidney expression data sets with the human tubulointerstitial compartment, because the tubulointerstitial compartment constitutes  $>95\%$  of total kidney mass, driving the majority of the signatures obtained from the mouse tissue. In addition, tubulointerstitial inflammatory lesions and fibrosis correlate with the decrease in renal function in LN and are markers of poor outcome (33–36).

The strategy used for cross-species shared transcriptional network analysis is depicted in Fig. 1. A sequential knowledge-extraction approach was applied first to generate a transcriptional network that integrates differential gene expression with public knowledge of gene interactions and automated promoter analysis to define transcriptional dependencies in each data set. Next, conservation of regulatory network elements was tested using a suboptimal graph matching approach (TALE) developed by Tian and Patel (28). TALE identifies core network elements shared between two data sets. TALE tolerates a predefined degree of mismatches in network substructure during consensus network generation, a critical feature shown to be robust for identifying the cross-species differences seen in many regulatory pathways between mouse and man. In the human–mouse comparison of LN, the NZM2410 glomerulosclerotic mouse model showed the highest number of cross-species conserved regulatory hubs (nodes) identified by TALE, followed by the NZB/W model and the NZW/BXSB model. The number of shared nodes was 125 (Fig. 2A), 86 (Fig. 2B), and 67 (Fig. 2C), respectively. Of these, 81 for the NZM2410 model, 62 for the NZB/W model, and 52 for the NZW/BXSB model were regulated in the same direction as in

Table I. Number of genes regulated among the groups compared in mouse models and human and overlapping with human data sets

| Mouse Model | Groups Compared                         | Genes Regulated <sup>a</sup> | Corresponding Human Orthologous Genes | Overlap with 3159 Genes <sup>a</sup> Regulated in Human Glomerular LN <sup>b</sup> | Overlap with 2261 Genes <sup>a</sup> Regulated in Human Tubulointerstitial LN <sup>b</sup> | Genes Regulated in Murine and Human LN in Both Renal Compartments <sup>b</sup> |
|-------------|---|------------------------------|---------------------------------------|--|--|--|
| NZB/W       | 23-wk Pre-N compared with 16-wk control | 234                          | 203                                   | 58   | 56   | 29   |
|             | 23-wk N compared with 16-wk control     | 919                          | 826                                   | 315  | 242  | 177  |
|             | 23-wk N compared with 23-wk Pre-N       | 1382                         | 1227                                  | 375  | 309  | 200  |
|             | 36-wk N compared with 23-wk Pre-N       | 2642 <sup>c</sup>            | 2442                                  | 631  | 379  | 242  |
| NZM2410     | 36-wk N compared with 16-wk control     | 3201                         | 2972                                  | 674  | 385  | 244  |
|             | 30-wk N compared with 7-wk control      | 4015 <sup>c</sup>            | 3727                                  | 699  | 467  | 251  |
|             | 17-wk Pre-N compared with 8-wk control  | 319                          | 302                                   | 95   | 79   | 48   |
|             | 18–21-wk N compared with 8-wk control   | 1877                         | 1757                                  | 568  | 384  | 246  |
| NZW/BXSB    | 18–21-wk N compared with 17-wk Pre-N    | 2900 <sup>c</sup>            | 2652                                  | 622  | 447  | 268  |

<sup>a</sup>*q* value < 0.05 and fold change ≥ 1.2 for the upregulated genes and ≤ 0.8 for the downregulated genes.  
<sup>b</sup>Genes regulated in same directionality in regulation.  
<sup>c</sup>Groups with highest level of shared nodes in network analysis used for further studies.  
N, Nephritic (proteinuria > 300 mg/dl, histologic nephritis score > 2); Pre-N, pre-nephritic (serum autoantibodies, proteinuria ≤ 100 mg/dl, histologic nephritis score ≤ 2).

the human samples. The lists of nodes and their regulation in each species are provided in Supplemental Table II.

Twenty nodes (19 induced and 1 repressed) were common to the three LN murine models and humans and regulated in the same direction (Fig. 2D, 2E, Supplemental Table II). These nodes mainly reflect transcripts associated with cellular infiltration and activation and included genes involved in signal transduction (*STAT1*, *LYN*, *ANXA2*), cytokines/chemokines (*CCL5*, *CXCL10*), cellular reorganization/traffic (*RAB8B*, *VIM*), cell surface markers (*PTPRC*, *TLR2*, *CD44*), and Ag-presentation/processing (*B2M* and inducible immunoproteasome subunits *PSMB8*, *PSMB9*). Three nodes were related to extracellular matrix/glomerular basement membrane/fibrosis (*FN1*, *COL18A1*, *TIMP1*). An increase in lysozyme (*LYZ*) is most likely reflective of proximal tubular damage. Finally, four nodes reflected endothelial cell activation (*VCAM1*), fibrinolysis (*ANXA2*), coagulation (*F2R* - thrombin receptor *PAR1*), and decreased angiogenesis (*VEGF-A*) (Fig. 2A). A decrease in VEGF-A expression was confirmed at the protein level in the glomerular compartment of patients with LN compared with control biopsies or biopsies from patients with vasculitis and a similar degree of kidney function (37). *F2R* (thrombin receptor *PAR1*), *FN1*, *LYN*, and *VEGFA* represented the main nodes of the transcriptional network built based on the literature knowledge, identifying these molecules as core elements in the shared regulatory network across models and species (Fig. 2E).

Pathway analysis of the genes regulated in the same direction from each cross-species conserved network further confirmed these findings, because the top pathways that were shared among the three models and human LN interstitium reflected innate and adaptive immune activation, immune cell infiltration, and tissue remodeling (Table II, Supplemental Table III). In addition, upregulation of Ig genes was observed in all three models (particularly the NZB/W model) and in human LN, reflecting B cell and plasma cell infiltration. These genes did not appear in the TALE or ingenuity analyses because of species differences in the Ig repertoire.

TALE consensus networks generated from the comparison of the three mouse models and the glomerular human LN data set are provided in Supplemental Fig. 1. Similar to the results for the tubulointerstitial compartment, NZM2410 mice shared the most nodes with human LN, and 24 nodes, representing a prominent macrophage/DC signature, were shared among all three models and LN.

Of the three models, the sclerotic kidneys of NZM2410 mice shared the most renal transcriptional events with human LN tubulointerstitium. Of the 125 shared nodes between NZM2410 mice and human LN kidneys and excluding the 20 common genes described above, 61 were regulated in the same direction (22 were downregulated and 39 were upregulated) (Supplemental Table II). The downregulated nodes included many genes involved in cholesterol metabolism, as well as genes involved in solute transport, consistent with the loss of differentiated tubular cell function. The upregulated nodes reflected tissue-injury processes (apoptosis, fibrosis, coagulation, tissue remodeling); expression of proteases, kinases, and protease inhibitors; and IFN-induced genes (Supplemental Table II).

Each of the other two models shared unique nodes with human LN interstitium. The NZB/W mouse, with diffuse proliferative glomerulonephritis, shared 86 nodes with the human LN kidneys. Excluding the 20 shared genes described above, 42 of them were regulated in the same direction in both NZB/W mice and human tubulointerstitium (27 upregulated and 15 downregulated). Eighteen nodes were shared only by the NZB/W mice and human LN and included *IFI30*, *CXCR4*, and *CCL9* (Supplemental Table IID). Many of the nodes unique to this human–NZB/W comparison

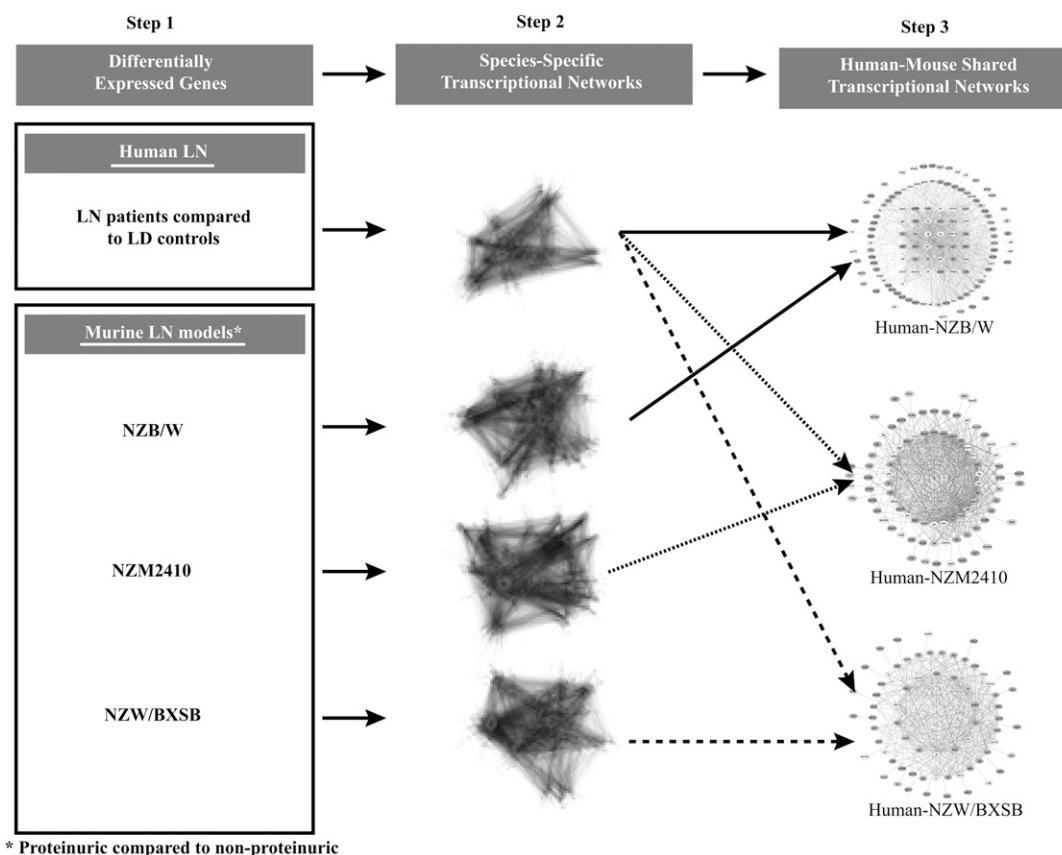


**FIGURE 1.** Analytical strategy of cross-species shared tubulointerstitial transcriptional networks using TALE. Individual transcriptional networks were generated using the literature-based Genomatix BiblioSphere software and were overlapped using TALE to define cross-species shared transcriptional networks.

reflected lymphocyte infiltration and activation, a feature of human LN not found in NZM2410 mice.

The NZW/BXSB mouse, with severe proliferative glomerulonephritis, shared the least number of nodes with human LN tubulointerstitium (67 nodes). Excluding the 20 genes in common with the two other models, as described above, 32 nodes were regulated in the same direction as in human disease (26 upregulated and 6 downregulated). Seventeen genes were shared exclusively by the NZW/BXSB mice and human LN (Supplemental Table IID). Unique nodes in this mouse included *Muc1*, *Nid2*, and *Matn1*, which are involved in extracellular matrix formation; the DC-derived chemokine *CXCL3*; and *IRF7*, likely reflecting the increase in TLR signaling that occurs both in this mouse and in human LN.

The gene-expression pattern that we describe in this study in patients with LN might also be shared with other inflammatory renal diseases. To address this point, microarray data from ERCB cohorts available to the investigators as part of an independent study (W. Ju et al., submitted for publication) were compared with the LN data. Gene-expression data from glomeruli and tubulointerstitial compartments of the inflammatory disease IgAN and the noninflammatory disease HT were compared with the human/mouse overlapping gene-expression profiles shown in Table I. For these comparisons, we focused on NZB/W and NZM2410 mouse models, because they share most features with the human disease. As shown in Fig. 3, a significant proportion of transcripts was found to be regulated in an LN-specific manner (26–39% of the regulated genes in LN). As expected, more inflammatory genes were shared with the IgAN biopsies than with the HT biopsies. Interestingly, the LN glomeruli had more downregulation of *VEGFA* and of mitochondrial genes (citrate synthase node) than

did the IgAN or HT biopsies (Fig. 3A), suggesting a greater degree of oxidative stress in the LN biopsies. The LN interstitium had a more prominent type I IFN signature (*CXCL10* node) and more evidence of procoagulant activity (*THBS1* node) than did the IgAN or HT biopsies (Fig. 3B, data not shown).

#### Renal LN macrophage functional analysis

A key feature of the cross-species comparison in LN was the concordant regulation of macrophage/DC transcripts, with a prominent Ag-presentation and pattern-recognition receptor signature shared between mouse and man (Table II, Supplemental Table IIIA). Mononuclear phagocytic cells have been extensively described as key players in both acute and chronic kidney diseases (38–40); however, to our knowledge, no study has analyzed the macrophage transcriptome within the kidneys of LN patients. Purifying small subpopulations of cells from human LN kidney biopsies is technically challenging because of the limited amount of kidney tissue available from renal biopsy cores. Therefore, we applied a cross-species integration strategy of defining the transcriptome of the renal mononuclear phagocytes from nephritic mouse kidneys and using these data to define potential macrophage/DC-derived genes from SLE biopsy samples. For an overview of the strategy used, see Fig. 4.

We previously showed in all three mouse models that activation of mononuclear phagocytes associated with upregulation of CD11b on CD11b/F4/80<sup>hi</sup>/CD11c<sup>int</sup> intrinsic renal “macrophages” (F4/80<sup>hi</sup> cells) is a cardinal feature of new-onset proteinuria (14, 17, 18). Furthermore, in all three models, F4/80<sup>hi</sup> cells are the dominant mononuclear phagocyte population both in prenephritic and nephritic kidneys (14, 17, 18). Although cells from the NZM2410 mouse kidneys, which share the most number of nodes with the



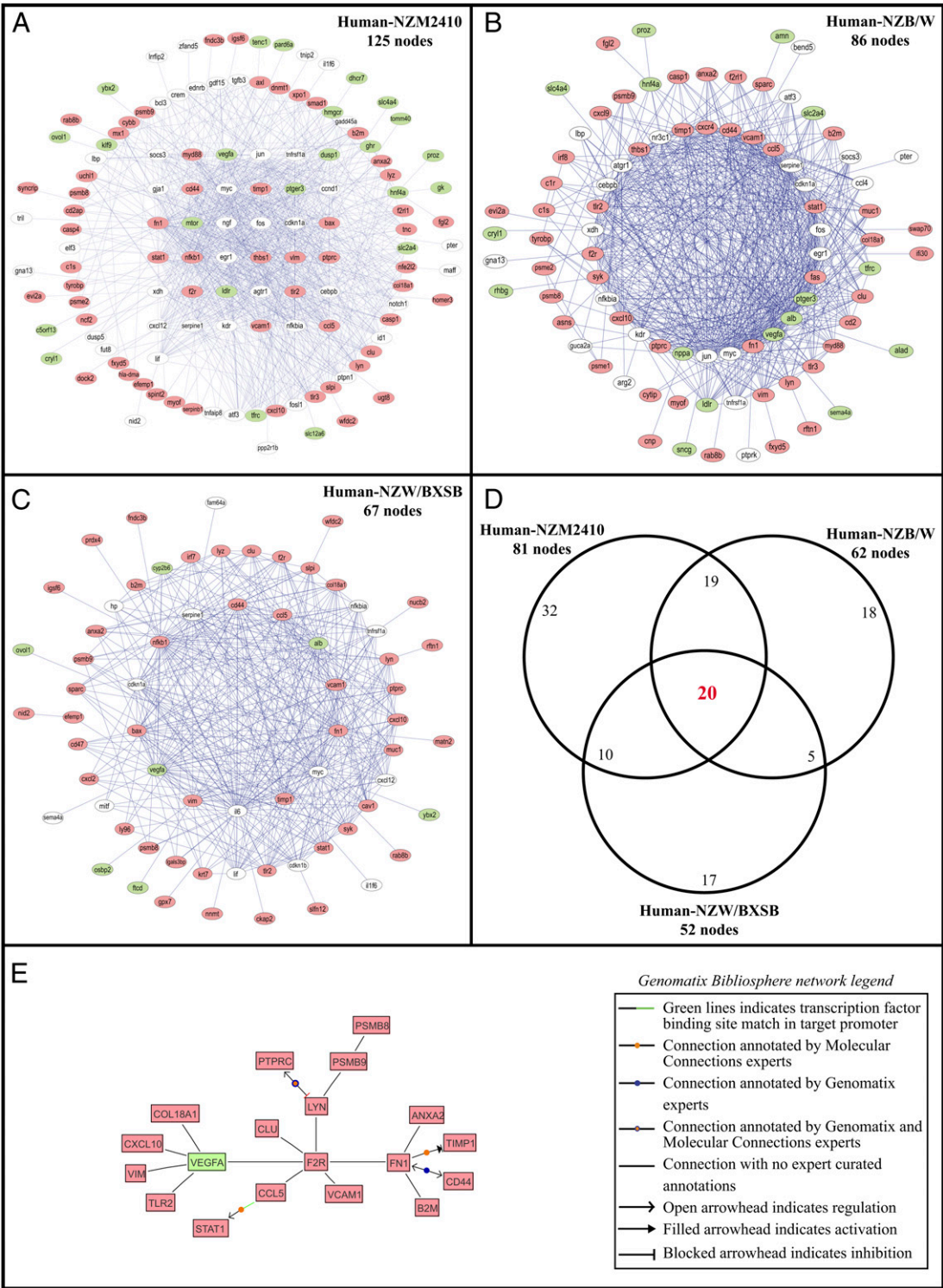


**FIGURE 2.** Human–mouse shared tubulointerstitial transcriptional networks. Networks sharing the most connections between human LN and NZM2410 (nephritic versus young control; 125 nodes) (**A**), NZB/W (36 wk with established nephritis versus 23 wk pre-nephritic; 86 nodes) (**B**), and NZW/BXSB (nephritic versus pre-nephritic; 67 nodes) (**C**). (**D**) Overlap of the nodes between the three comparisons, using only the nodes regulated in the same direction in both species in each network (81/125 nodes in the NZM2410 model, 62/86 nodes in the NZB/W model, and 52/67 nodes in the NZW/BXSB model). Each node represents a gene; each edge (blue line) represents a connection between two nodes. The nodes having >20 connections, 2–19 connections, and only 1 connection are displayed in the inner layer, the middle layer, and the outside layer, respectively. The nodes upregulated in both species, down-regulated in both species, or discordantly regulated among species are shown in red, green, and white, respectively. (**E**) Transcriptional Genomatrix Biblosphere network from the 20 overlapping nodes of the TALE results.

human LN tubulointerstitium, might provide the most information, these mice have far fewer F4/80<sup>hi</sup> cells than do the other two strains and die almost as soon as they become proteinuric (18). Therefore, we used the transcriptome from isolated F4/80<sup>hi</sup> cells from NZB/W kidneys as a probe for the human samples. Gene-expression array data from these cells were reported previously (17). A total of 2506 genes was differentially regulated in F4/80<sup>hi</sup> cells isolated from kidneys from nephritic mice compared with

Table II. Top canonical pathways significantly regulated ( $p < 0.05$ ) from the genes shared and regulated in the same direction in human LN (LN versus LD) tubulointerstitium and in each mouse model (nephritic versus prenephritic), as assessed by Ingenuity Pathway Analysis

| Canonical Pathways<br>(No. of Genes in Pathway)                                   | NZM2410 (467 Genes) |                |                                  | NZB/W (379 Genes) |                |                                  | NZW/BXSB (447 Genes) |                |                                  |
|---|---------------------|----------------|----------------------------------|-------------------|----------------|----------------------------------|----------------------|----------------|----------------------------------|
|   | Rank                | <i>p</i> Value | Regulated Genes in Pathway (No.) | Rank              | <i>p</i> Value | Regulated Genes in Pathway (No.) | Rank                 | <i>p</i> Value | Regulated Genes in Pathway (No.) |
| Ag-presentation pathway (43)  | 1                   | 2.0E-09        | 12                               | 1                 | 1.2E-11        | 13                               | 1                    | 1.2E-09        | 12                               |
| Role of pattern recognition receptors in recognition of bacteria and viruses (87) | 2                   | 8.5E-08        | 15                               | 5                 | 6.8E-09        | 15                               | 2                    | 6.6E-09        | 16                               |
| OX40-signaling pathway (90)   | 3                   | 2.6E-07        | 12                               | 8                 | 3.3E-08        | 12                               | 3                    | 1.7E-07        | 12                               |
| CTL-mediated apoptosis of target cells (81)                                       | 4                   | 6.2E-07        | 11                               | 2                 | 6.3E-10        | 13                               | 4                    | 4.2E-07        | 11                               |
| Th cell differentiation (72)  | 5                   | 7.9E-07        | 13                               | 13                | 7.1E-07        | 12                               | 5                    | 5.1E-07        | 13                               |
| Allograft rejection signaling (91)  | 6                   | 1.9E-06        | 10                               | 3                 | 2.2E-09        | 12                               | 6                    | 1.4E-06        | 10                               |
| DC maturation (188)   | 7                   | 2.8E-06        | 19                               | 4                 | 5.6E-09        | 21                               | 8                    | 1.5E-06        | 19                               |
| Type I diabetes mellitus signaling (121)  | 8                   | 2.9E-06        | 16                               | 9                 | 2.4E-07        | 16                               | 9                    | 1.7E-06        | 16                               |
| Cdc42 signaling (174)   | 9                   | 3.4E-06        | 17                               | 10                | 2.5E-07        | 17                               | 12                   | 8.8E-06        | 16                               |
| Autoimmune thyroid disease signaling (61)   | 10                  | 7.9E-06        | 9                                | 6                 | 1.1E-08        | 11                               | 11                   | 5.7E-06        | 9                                |
| Graft-versus-host disease signaling (50)  | 11                  | 1.6E-05        | 9                                | 7                 | 3.0E-08        | 11                               | 13                   | 1.2E-05        | 9                                |
| Complement system (35)  | 13                  | 2.5E-05        | 8                                | 15                | 6.2E-06        | 8                                | 10                   | 1.9E-06        | 9                                |
| Hepatic fibrosis/hepatic stellate cell activation (147)                           | 16                  | 3.7E-05        | 17                               | 17                | 1.3E-05        | 16                               | 7                    | 1.4E-06        | 19                               |

those from  $\leq 16$ -wk-old NZB/W mice without any renal disease ( $q$  value  $< 0.05$ , fold change  $\geq 1.2$  for the upregulated genes and  $\leq 0.8$  for the downregulated genes) (Fig. 4A).

To analyze whether this murine renal F4/80<sup>hi</sup> intrinsic macrophage signature is present in human LN kidneys, we compared the regulated murine renal F4/80<sup>hi</sup> genes with the genes that were differentially expressed in the tubulointerstitium and glomeruli of patients with LN compared with LD controls. A total of 213 murine macrophage genes was regulated in the same direction as in the human tubulointerstitium, and 334 macrophage genes were concordantly regulated in human glomeruli (Fig. 4B). Literature-based networks were generated from these 213 “tubulointerstitial LN macrophage/DC genes” and 334 “glomerular LN macrophage/DC genes” for further interpretation.

A total of 110 macrophage/DC genes was expressed in both tubulointerstitium and glomeruli of human LN biopsies (Fig. 4B) and were dominated by a type I IFN signature with both *MyD88* and *IRF7* nodes (Fig. 4B, lower panel). This signature included *MDA-5* (*IFIH1*) and *Viperin* (*RSAD2*), genes involved in nucleic acid sensing and the IFN pathway. Fourteen of the “macrophage” genes found in both human renal compartments had a binding site for the transcription factor IRF7 in their promoter, as assessed by Genomatrix (Table III), suggesting a role for TLR activation in tissue injury (30). Other concordantly induced genes included the src family kinases *Hck* and *Lyn*, the chemokine receptor *CXCR4*, complement factor *C3*, and *Factor B*, an important amplifier of complement activation through the alternative complement pathway. Myc transcription factor consensus binding sites were significantly enriched in the promoter regions of macrophage genes; concordant with this observation, the transcriptional repressor *Myc* was found to be downregulated in the isolated murine F4/80<sup>hi</sup> cells.

A total of 224 unique “macrophage” genes was expressed in the glomerular profile from human LN biopsies. In this compartment, *PPAR $\gamma$* , *MMP2*, and the CD11b  $\alpha$ -chain *ITGAM* were key nodes in the transcriptional network (Fig. 4B). *PPAR $\gamma$*  binding sites were enriched in promoter regions of 25 glomerular macrophage genes, further supporting a role for this transcriptional activator in macrophage transcript regulation in LN (Table III). Multiple phagocytic receptors were upregulated in the glomerular profile

(*Trem2*, *MERTK*, and *TGM2*), as well as tissue repair genes (*MMP2*, Heparanase, the anti-oxidant *HMOX1*, and *SMAD7*) and proinflammatory genes (*Trem1*, *FPRI*, *CD40*). Induction of multiple elements of the proteasome resulted in “protein ubiquitination” being scored as the top ranking pathway (Supplemental Table IIIB) found in the shared transcriptome induced in both murine LN macrophages and glomeruli from human LN.

One hundred and three “macrophage” genes were shared with the genes differentially regulated in the LN tubulointerstitium and included molecules from the coagulation and fibrinolytic systems: *F2R*, *Serpine 2* (*PAI-1*), *TNC*, *THBS1*, and *ANXA5* (Fig. 4B). Transcription factor-binding analysis indicated a significant enrichment of NF- $\kappa$ B binding sites in promoter regions of the shared regulated transcripts (Table III).

In sum, the comparative analysis of murine-derived transcriptome of renal macrophages with human LN signatures allowed us to define transcriptional networks operating ubiquitously in LN, including IRF7-dependent transcripts, as well as those operating in distinct microenvironments. Signatures of glomerular-resident macrophages showed a specific enrichment for *PPAR $\gamma$* -dependent regulation, whereas tubulointerstitial macrophages showed a predominance of NF- $\kappa$ B-dependent transcripts.

Much of the data from the macrophages of NZB/W mice was validated previously using real-time RT-PCR (17), and real-time RT-PCR data for whole kidneys from each of the three mouse strains will be reported separately (R. Sahu, R. Bethunaickan, O. Edegbe, and A. Davidson, manuscript in preparation). Human microarray data were validated by processing TaqMan real-time PCR on tubulointerstitial samples from an independent cohort for several of the specific genes of interest described above (Table IV; Supplemental Table I). Because glomerular material is very limited, we focused validation on the most relevant gene (*ITGAM*) in these samples (Table IV). All genes evaluated by RT-PCR were significantly regulated, with high fold change in LN compared with healthy pretransplant LDs (fold change between 1.48 and 22.21,  $p < 0.05$ ), with the exception of *CD14*, *CXCR4*, and *GPMB*, for which there was a trend toward upregulation, as observed in the arrays. TaqMan real-time PCR was also performed on a subset of 9 LN from the 32 LN used on arrays and 6 LDs. All



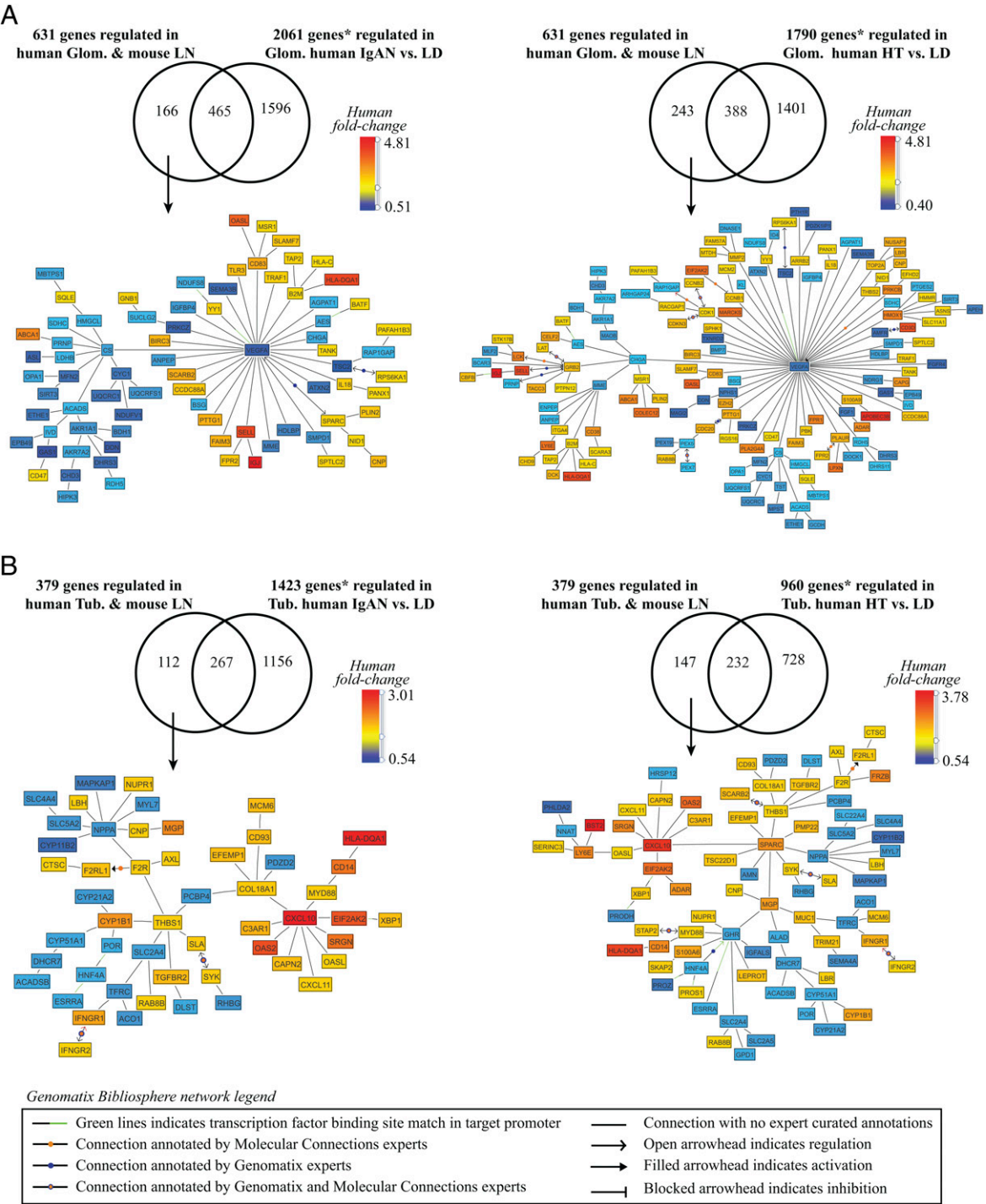


**FIGURE 3.** Human–NZB/W mouse LN comparison with IgAN and HT. **(A)** Glomerular compartment. **(B)** Tubulointerstitial compartment. The figures display the transcriptional networks (Genomatrix BiblioSphere) obtained from the genes that were co-cited in PubMed abstracts in the same sentence linked to a function word (B2 filter) (145 of 166 genes [(A), left panel]; 220 of 243 genes [(A), right panel]; 104 of 112 genes [(B), left panel]; 138 of 147 genes [(B), right panel]). LN-regulated transcripts were mapped into the transcriptional networks and included in the comparison. \**q* value < 0.05 and fold change ≥ 1.2 for the upregulated genes and ≤ 0.8 for the downregulated genes.

genes were significantly upregulated in this technical replicate (data not shown).

*Immunohistochemical staining of kidneys*

To illustrate differences between mononuclear cells in micro-compartments of the human kidney, a series of 10 biopsies with LN was compared with 5 biopsies of pretransplant controls (Fig. 5). Immunohistochemistry for DC-SIGN (CD209), the myeloid DC marker S100, and the macrophage scavenger receptor CD68 was

performed in human LN (Fig. 5). As predicted by the transcriptional analysis, SLE patients had an increase in cells staining with all three markers. CD68<sup>+</sup> cells were found both within the glomeruli and in the interstitium, whereas DC-SIGN<sup>+</sup> cells were restricted to the interstitium. S100<sup>+</sup> cells were loosely scattered in both glomeruli (circulating cells within glomerular capillaries) and the interstitium. These findings confirm our hypothesis generated from the transcriptional data that distinct renal mononuclear phagocytes infiltrate the different intrarenal compartments in human LN.

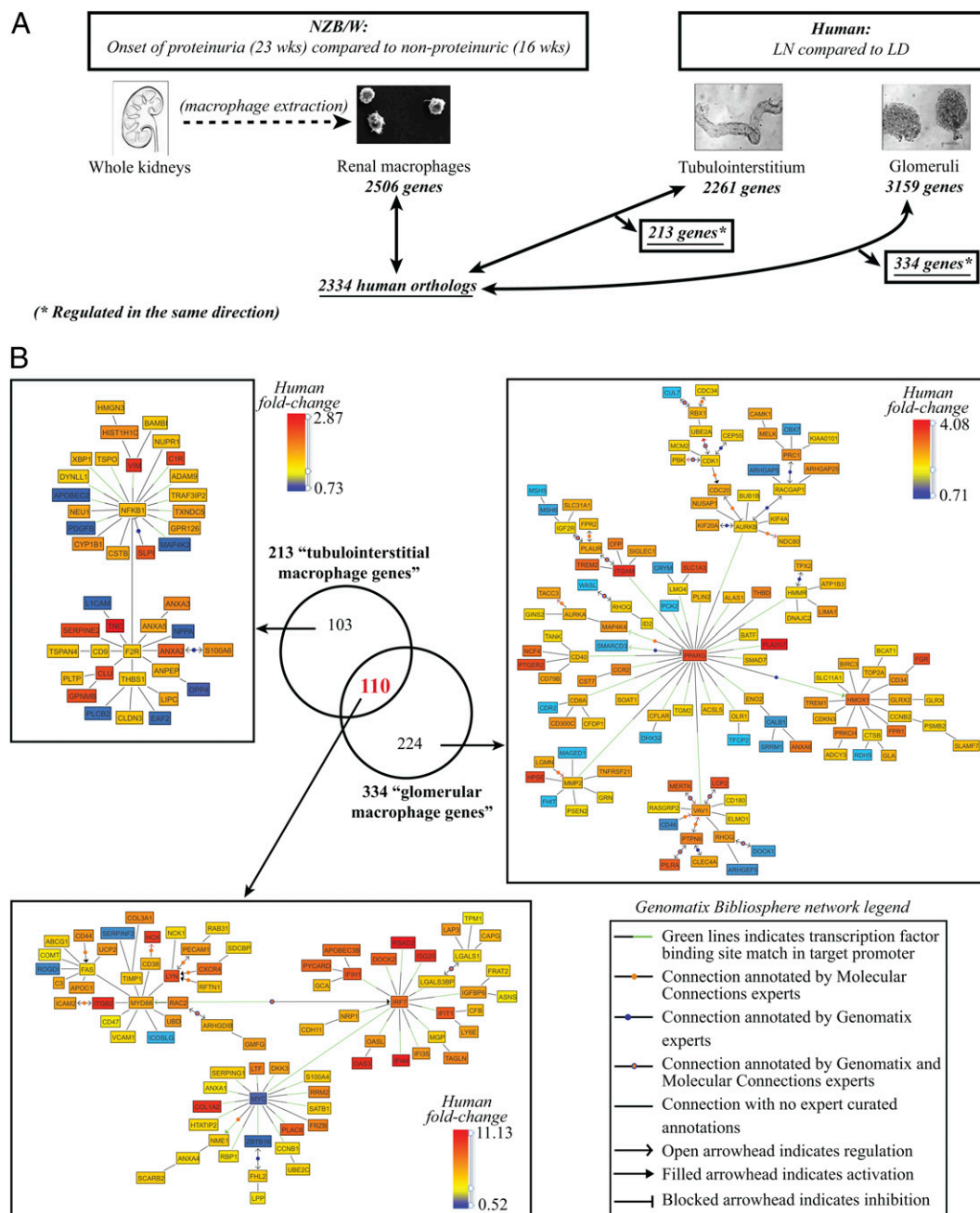


**FIGURE 4.** Renal LN F4/80<sup>hi</sup> intrinsic functional analysis. **(A)** Analytical strategy of renal LN “macrophage” functional analysis ( $q$  value  $< 0.05$ , fold change  $\geq 1.2$  for the upregulated genes and  $\leq 0.8$  for the downregulated genes). **(B)** Overlap of the defined tubulointerstitial and glomerular “macrophage genes.” Transcriptional networks were generated using the literature-based Genomatrix BiblioSphere software from the 103 tubulointerstitial-restricted genes, the 224 glomerular-restricted genes, and the 110 genes shared by both compartments and mouse F4/80<sup>hi</sup> intrinsic macrophages ( $q$  value  $< 0.05$ , fold change  $\geq 1.2$  for the upregulated genes and  $\leq 0.8$  for the downregulated genes). Respectively, the pictures display the 42 of 103, 78 of 110, and 120 of 224 genes that were co-cited in PubMed abstracts in the same sentence linked to a function word (B2 filter).

In sum, our data suggest that there are different functional features of various mononuclear phagocytic populations that infiltrate different renal microenvironments in LN.

## Discussion

Although much of the focus in the classification of human lupus has been on the glomerulus, there is an increasing understanding that renal outcomes correlate best with the degree of tubulointerstitial inflammation and damage (33–35). After the deposition of immune complexes in the glomerulus, periglomerular macrophages may be attracted by locally produced chemokines or may be activated by inflammatory mediators to proliferate in situ. In addition, because

the effluent blood flow from the glomerulus provides the sole blood supply for peritubular capillaries, glomerular hypertension and hypertrophy compromise peritubular blood flow, resulting in hypoxia, tubular activation, and tubular epithelial cell death. This induces resident macrophage activation and peritubular inflammation and is associated with tissue remodeling, fibrosis (33), and finally, irreversible renal damage. Release of damaged tissue, cytokines, and other inflammatory mediators amplify the inflammatory process. These effector inflammatory processes are likely to be shared between individuals and may be addressed therapeutically.

Therefore, our study had two major goals. The first was to identify common expression profiles that reflect renal events shared

Table III. Transcription factor analysis from the defined “tubulointerstitial and glomerular macrophage genes,” as assessed by Genomatrix BiblioSphere software

|  |        |          |          |          |          |         |        |
|--|--------|----------|----------|----------|----------|---------|--------|
| 25 genes from the 224 “glomerular-restricted macrophage genes” having a binding site for PPARG (V\$PERO) in their promoter         | HMOX1  | CCR2     | SOAT1    | ID2      | ALAS1    | ITGAM   | ACSL5  |
| From the 110 “shared tubulointerstitial and glomerular macrophage genes”   | HMMR   | ENO2     | VAV1     | BATF     | PLIN2    | CD40    | AURKB  |
|  | MMP2   | MAP4K4   | CD8A     | OLR1     | SMAD7    | CFLAR   | PLA2G7 |
|  | PCK2   | TGM2     | SMARCD3  | LMO4     |          |         |        |
|  | MGP    | MYC      | DOCK2    | IFI35    | LGALS3BP | ISG20   | OASL   |
| 14 genes having a binding site for IRF7 (V\$IRFF) in their promoter  | MYD88  | IGFBP6   | IFT1     | IFIH1    | RSAD2    | IFI44   |        |
|  | NRP1   |          |          |          |          |         |        |
|  | NCK1   | S100A4   | FAS      | SERPING1 | CD44     | LGALS1  | ANXA1  |
| 27 genes having a binding site for MYC (V\$EBOX) in their promoter   | DKK3   | VCAM1    | LTF      | TIMP1    | CXCR4    | PLAC8   | CD38   |
|  | LYN    | ZBTB16   | COL1A2   | RRM2     | NME1     | CCNB1   | HCK    |
|  | MYD88  | SATB1    | IRF7     | RBP1     | LGALS3BP | HTATIP2 |        |
| 24 genes from the 103 “tubulointerstitial-restricted macrophage genes” having a binding site for NFKB1 (V\$NFKB) in their promoter | S100A6 | NPPA     | C1R      | ANXA2    | APOBEC2  | XBPI    | DPP4   |
|  | THBS1  | SERPINE2 | TRAF3IP2 | TXNDC5   | GPR126   | PDGFB   | TNC    |
|  | MAP4K2 | VIM      | TSPO     | ADAM9    | ANXA5    | DYNLL1  | CLU    |
|  | LICAM  | CD9      | ANXA3    |          |          |         |        |

between the three murine models and human LN. Defining such common pathways between mouse models and human diseases will most likely result in therapeutic targets with broad specificity. Our second goal was to define which molecular pathways found in the three disparate murine models with proliferative (NZB/W and NZW/BXSB) or sclerotic (NZM2410) glomerulonephritis are shared with human LN. This will facilitate experimental studies in murine LN models by allowing the a priori selection of the model system most closely mimicking the human LN situation for the specific pathway under interrogation. Our study showed that the sclerotic kidneys of NZM2410 mice shared most renal transcriptional events with human LN kidneys, but it also identified unique features of each of the murine models that were shared with human LN, stressing the need to have multiple model systems with matching molecular data available for further experimental validation of human LN pathways.

Transcriptional analyses of human and mouse kidneys with LN and proteinuria using TALE allowed us to extend our analysis beyond a simple gene–gene comparison by overlapping transcriptional networks from the two different species and then defining shared functional relationships. This analysis showed that macrophages/DCs are key players in the development of LN disease. The small amount of tissue obtained from kidney biopsies is a limitation for studying the role of isolated cell populations in the pathogenesis of human LN disease. The strategy of analyzing gene-expression profiles from infiltrating macrophage populations obtained from mouse kidneys allowed us to attribute mRNA signature to those cells in the human samples, even when such information might not be derived from the human tissue homogenate initially. These studies suggest differences in functional activities between mononuclear phagocytes in different renal subcompartments.

*The shared transcriptional profile*

Using TALE analysis, we identified 20 common transcriptional network nodes that were shared by all three LN murine models and the tubulointerstitium of human LN and regulated in the same direction. These nodes reflect key processes in chronic renal injury in SLE nephritis (i.e., immune cell infiltration and activation, macrophage and DC activation, endothelial cell activation, and damage and tissue remodeling/fibrosis), which were confirmed by pathway analysis.

Of the three models, the sclerotic kidneys of NZM2410 mice shared most renal transcriptional events with human LN kidneys. Histologically, the kidneys of NZM2410 mice have a limited degree of inflammation and more glomerulosclerosis than do those of the other two strains (12). The greatest similarity of this model to human LN may reflect the possibility that patients, in contrast to the murine models, accumulate significant chronic end-organ damage before they are referred to a nephrologist and undergo renal biopsy. In addition, most patients have already been treated, to some extent, by the time biopsies are performed, thus repressing the severity of acute inflammation compared with the untreated mouse models. Thus, the NZM2410 mouse may be an appropriate mouse model for testing add-on therapies directed at chronic progression of LN.

Most of the transcriptional network nodes unique to the NZB/W mouse, with diffuse proliferative glomerulonephritis, reflected lymphocyte infiltration and activation, a feature found in many SLE biopsies; this feature of nephritis is not found in NZM2410 mice. In particular, the expression of *CXCR4* was elevated; this chemokine receptor is expressed on plasma cells in mice, it is overexpressed on multiple leukocyte subsets in active lupus patients, and its ligand CXCL12 is overexpressed in human LN kidneys (41, 42). Tubu-



Table IV. TaqMan real-time PCR of selected genes of interest as validation of microarrays data

| Compartment        | Gene   | Microarrays |                | Real-Time PCR |                |
|--------------------|--------|-------------|----------------|---------------|----------------|
|                    |        | Fold Change | <i>q</i> Value | Fold Change   | <i>p</i> Value |
| Tubulointerstitium | CCR1   | 1.29        | 0.004          | 2.18          | 0.047          |
|                    | CD14   | 1.81        | 0.001          | 1.48          | 0.332          |
|                    | CCL5   | 1.81        | 0.001          | 12.81         | 0.049          |
|                    | CTSS   | 1.86        | 0.000          | 10.57         | 0.001          |
|                    | CXCL10 | 3.01        | 0.000          | 16.20         | 0.003          |
|                    | STAT1  | 3.62        | 0.000          | 9.28          | 0.000          |
|                    | CXCR4  | 1.86S       | 0.001          | 1.95          | 0.237          |
|                    | IRF7   | 1.66        | 0.000          | 6.99          | 0.002          |
|                    | HCK    | 1.37        | 0.000          | 3.35          | 0.003          |
|                    | LYN    | 1.63        | 0.000          | 2.54          | 0.009          |
|                    | CFB    | 2.74        | 0.000          | 5.22          | 0.000          |
|                    | IFI44  | 10.16       | 0.000          | 22.21         | <0.0001        |
|                    | GPXMB  | 2.10        | 0.000          | 3.36          | 0.058          |
| Glomeruli          | ITGAM  | 3.21        | 0.000          | 3.82          | 0.009          |

The comparison of LN versus LD represents the fold change.

linterstitial inflammation with lymphoid aggregates that may include germinal centers and abundant plasma cells is commonly found in human LN and is associated with worse renal outcome (43,

44). Indeed, a prominent Ig signature was found both in mouse kidneys and in the human tubulointerstitium. Compared with NZM2410 mice, there was less expression of nodes that included proteases, proapoptotic molecules, and extracellular matrix. Thus, this model appears to have more inflammation and less tissue remodeling than does the NZM2410 model.

The NZW/BXSB mouse model shared the least number of nodes with the human LN kidneys; surprisingly, given that both NZB/W and NZW/BXSB mice have severe proliferative disease, it overlapped less with the NZB/W mouse than it did with the NZM2410 mouse. This may reflect, as discussed above, the fact that human disease has most likely been treated to some extent. Unique nodes in this mouse were associated with extracellular matrix formation and myeloid cell activation, consistent with the large numbers of infiltrating myeloid cells in this model (14).

Several nodes were discordantly regulated in the murine models and human samples. These included nodes indicating a response to endoplasmic reticulum stress or hypoxia (*SERPINE1*, *EGRI*, *ATF3*, *MYC*, *CDKN1A*, *Fos*, and *Jun*) and genes that downregulate acute inflammatory cytokines (*SOCS3*, *ATF3*, *LIF*, *NFKBIA*). These findings suggest a greater degree of hypoxia in the mouse models than in human disease, perhaps reflecting the aggressive nature of untreated murine disease.

In summary, the three regulatory networks representing the transcriptional events shared among the human LN tubulointerstitium and kidneys of three LN mouse models showed significant overlaps, as well as characteristics specific to each model, each of which is shared with the human disease. These findings underscore the heterogeneity of LN and the pitfalls of extrapolating from a single mouse model to human disease. Our study illustrates the necessity of studying different mouse models, because specific questions about human disease might best be answered using a particular model. Importantly, the transcriptional profile highlighted a large number of genes associated with processes involved in chronic renal injury and disease progression that may be resistant to systemic immune suppression. Furthermore, comparison of the LN profiles with those of two other human renal diseases showed both similarities and differences. In particular, the differences between LN and IgAN reflected more prominent tissue hypoxia and tissue remodeling in the LN biopsies, features that might require a different type of therapeutic intervention to prevent a poor long-term outcome seen in LN. Our findings stress the need for including management strategies in SLE nephritis directed at slowing the progression of the renal impairment that may continue even after systemic inflammation has resolved.

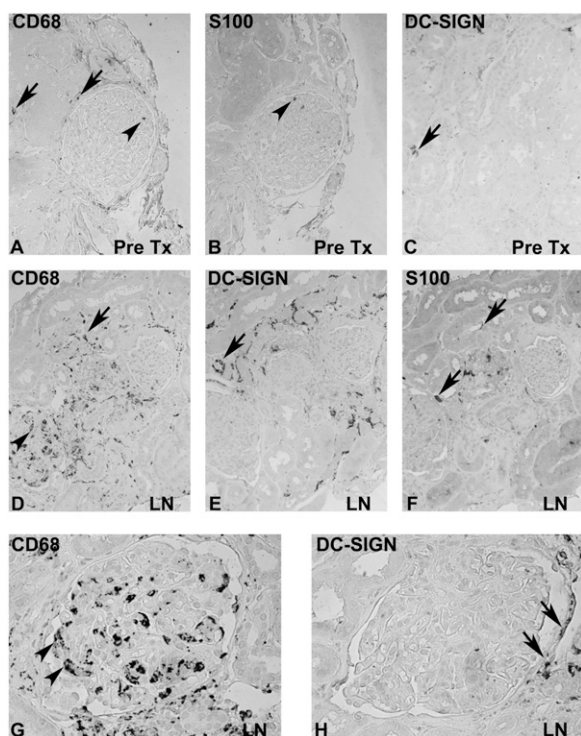


**FIGURE 5.** Localization of macrophage/DC markers in human LN. Immunohistochemistry for CD68 (**A, D, G**), S100 (**B, E**), and DC-SIGN (**C, F, H**) was performed on consecutive sections from a pretransplant biopsy (**A–C**) and biopsies of LN class IV (International Society of Nephrology/Renal Pathology Society 2003 classification) [original magnification  $\times 200$  (**A–F**),  $\times 400$  (**G, H**)]. Scattered CD68<sup>+</sup> cells (**A**) and lower numbers of S100<sup>+</sup> cells (**B**) were found in the tubulointerstitium (arrows) and occasionally in glomerular capillaries (arrowhead) in pretransplant biopsies. (**C**) A low number of DC-SIGN<sup>+</sup> cells was present in the tubulointerstitium (arrow). (**D–G**) In contrast, prominent numbers of CD68<sup>+</sup> and DC-SIGN<sup>+</sup> cells were present in biopsies from patients with LN. Consecutive sections demonstrate a prominent number of CD68<sup>+</sup> cells in glomerular capillaries (arrowheads), as well as a prominent accumulation of CD68<sup>+</sup> cells in the tubulointerstitium (arrows). (**H**) DC-SIGN<sup>+</sup> cells were restricted to the tubulointerstitium (arrows); no DC-SIGN was expressed on glomerular CD68<sup>+</sup> cells.

This approach has a number of intrinsic limitations. First, TALE was designed to provide the similarities between large networks (from two species in this study). Indeed, it aligns networks to define the conserved network. By definition, “approximate large graph matching” is useful because it has a defined mismatch tolerance and, thereby, can build a consensus signature; however, this feature is not optimized to define differences between networks. Second, because our transcriptional network generation integrates differential gene expression with automated promoter analysis and natural language processing using PubMed abstracts, it is biased toward the current literature, thereby enriching for known biological interactions between transcripts. Third, because most of the patients had experienced some type of treatment at the time of biopsy, leading to treatment-induced alterations of the expression profiles, they may not display the natural disease history observed in the murine models, masking important aspects of disease pathogenesis. Despite these constraints, our study identified a prominent macrophage/DC-activation signature as a key feature of all three lupus models and of human LN. Indeed, our study confirms a previous report (44) of a prominent myelomonocytic signature in the glomeruli of most LN patients, with expression of a set of genes similar to that identified in this study. Therefore, our findings suggest that further study of these cell types, their origins, and the mechanisms by which they become activated in the kidneys may yield new therapeutic strategies, as well as that mouse models, such as NZB/W, are suitable for performing these studies.

#### *The macrophage profile*

Pathway analysis of the shared nodes identified mononuclear phagocyte activation as a key player in LN. Therefore, we investigated the contribution of these cells to the total mRNA expression profile by comparing the human compartment-specific gene-expression profiles with the profile of the dominant F4/80<sup>hi</sup>-intrinsic macrophage population isolated from control and nephritic NZB/W kidneys. This strategy allowed us to detect transcripts of the macrophage signature in the heterogeneous human renal tissue.

Resident renal mononuclear phagocytes have variably been called resident or intrinsic renal macrophages or resident renal DCs (16). In mice, there are at least five subpopulations of these cells in the kidneys (R. Sahu and A. Davidson, manuscript in preparation) (17), but the major population that forms a network throughout the interstitium expresses high levels of F4/80, CD11b, intermediate levels of CD11c, and low/intermediate levels of Ly6C; it is positive for MHC class II but expresses low levels of costimulatory molecules (17). The generation of CX3CR1-GFP-labeled mice has allowed visualization of analogous CX3CR1<sup>+</sup> cells in a network surrounding glomerular tubules (45). These cells are capable of phagocytosis and constantly retract and extend dendritic processes into the interstitium (46, 47). Their role is probably a sentinel one under physiologic circumstances, but they can contribute to renal injury once activated. We recently showed that F4/80<sup>hi</sup>-resident renal cells increase in number in the periglomerular area and/or throughout the interstitium in all three lupus models during the course of the disease; they become activated with disease onset (17–19) and revert to their physiologic state upon induction of remission. The expression profile of these cells reveals a mixed functional signature, with both M1- and M2-like characteristics, which likely reflects exposure of SLE kidney-resident macrophages to multiple stimuli, including immune complexes, multiple cytokines, TLR signals, fibrinogen, dead and dying cells, hypoxia, and other danger signals. This aberrant activation profile is associated with chronic and progressive renal injury (17).

In humans, only limited phenotypic analyses of macrophages and DC have been performed (30, 48, 49), mostly using immunohistochemistry. Human tubulointerstitial CD68<sup>+</sup> mononuclear phagocytes have a mixed phenotype and include CX3CR1<sup>+</sup> cells and cells variably positive for the C-type lectins DC-SIGN and BDCA-1. As we show in this study, in SLE biopsies, CD68<sup>+</sup> cells infiltrate both the glomerular and the tubulointerstitial compartment; interestingly, however, the tubulointerstitial cells tend to be positive for DC-SIGN, whereas cells that accumulate in and around glomeruli are negative for DC-SIGN (49), suggesting potential functional differences between the two compartments. A previous study of gene expression of microdissected glomeruli from SLE patients revealed that nearly all lupus biopsies have a myelomonocytic-expression signature (44) that includes genes that we also detected in F4/80<sup>hi</sup> cells from nephritic kidneys. However, functional studies in humans are still lacking.

Our strategy allows us to separately assess the glomerular/periglomerular and tubulointerstitial compartments of human LN biopsy samples for genes that are regulated in activated renal mononuclear phagocytes from nephritic NZB/W mice. This strategy allows us to extract gene-expression patterns that reflect differences in expression rather than changes in cell number. The genes shared by murine activated F4/80<sup>hi</sup> macrophages and both human intrarenal compartments are dominated by a prominent type I IFN signature, activation of the alternative complement pathway through *Factor B*, and upregulation of the src family kinases *Hck* and *Lyn*, which are important effectors of integrin-mediated macrophage adhesion and FcR-mediated phagocytosis (47, 50–52). The chemokine receptor *CXCR4*, which is expressed by multiple leukocyte subsets in SLE kidneys (41, 42), is also highly upregulated. *CXCR4* blockade was reported to reduce renal leukocyte infiltration in murine LN (41, 53). Transcription factor analysis revealed a large number of genes regulated by the transcriptional repressor *Myc*, which, itself, is downregulated in the murine cells. Downregulation of *Myc* is associated with monocyte to macrophage differentiation, although the functional target genes are not well defined (54, 55).

Unique profiles of the “macrophage signature” in the glomerular and interstitial compartments also suggest functional differences. The 224 unique genes shared between the NZB/W macrophage signature and human LN glomeruli are dominated by a PPAR $\gamma$  transcriptional profile. PPAR $\gamma$  is expressed by alternatively activated macrophages, and it suppresses the production of inflammatory cytokines while inducing the production of IL-10 (56, 57); it also mediates phagocytosis of apoptotic material (58). PPAR $\gamma$  agonists decrease extracellular matrix accumulation and prevent renal macrophage accumulation in response to injury. PPAR $\gamma$ -deficient macrophages also fail to acquire an anti-inflammatory phenotype upon engulfment of apoptotic cells, suggesting a role for PPAR $\gamma$  in immune clearance. Several recent studies showed shown remarkably beneficial effects of PPAR $\gamma$  agonists in murine models of SLE nephritis, suggesting that these drugs could be appropriate therapies for preventing chronic renal damage in SLE (59, 60); our study suggests that these drugs may enhance a protective function of glomerular macrophages in humans as well. Other phagocytic receptors were also highly upregulated in the glomerular profile, suggesting that the glomerular macrophages are actively involved in phagocytosis as are the mouse F4/80<sup>hi</sup> cells (17). Pathway analysis revealed a significant enrichment of protein ubiquitination transcript regulation in glomeruli. We previously showed that F4/80<sup>hi</sup> cells from proteinuric NZB/W mice accumulate large numbers of autophagocytic vesicles (17). An increase in both protein ubiquitination and autophagy pathways, together with the increase in cell surface molecules involved in

phagocytosis, suggests an important role for these cells in intracellular proteolysis, presumably of oxidatively modified and ubiquitinated proteins. The glomerular “macrophage” profile also uniquely expressed a tissue repair signature, suggesting a role for these cells in tissue remodeling. Together, these data suggest that the glomerular mononuclear phagocyte is an actively phagocytic cell with potentially protective functions but that it may also contribute to aberrant tissue remodeling.

The unique tubulointerstitial-restricted “macrophage” signature was characterized by the expression of genes involved in the coagulation and fibrinolytic systems. Therefore, these genes might be useful as markers for the presence of tubulointerstitial infiltrates and possibly a risk for fibrosis in LN. Another gene highly expressed in the interstitium is *GPMB* (osteoactivin), which is upregulated during macrophage differentiation from monocytes and appears to function as a negative regulator of inflammation (61). Upregulation of osteoactivin was observed in monocytes obtained from uremic patients or in normal monocytes cultured in uremic serum (61), as well as in CD11b<sup>+</sup> cells within inflammatory myocardial infiltrates in a model of adverse myocardial remodeling (62). In addition, this compartment was characterized by a striking NF- $\kappa$ B transcriptional profile that was absent in the glomerular “macrophage” signature. In sum, these findings suggest that, although mononuclear phagocytes in different renal locations share some functional characteristics, the different microenvironments are associated with unique gene-expression profiles that may profoundly influence cell function.

Several genes that were highly upregulated in F4/80<sup>hi</sup> cells from NZB/W nephritic kidneys (17) were not regulated in human LN samples. Some of this discrepancy may have been due to the dilution effects of whole tissue versus purified cells (e.g., IL-10 expression was not regulated in whole mouse kidneys, although it was highly expressed in isolated F4/80<sup>hi</sup> cells from proteinuric mice). Nevertheless, these differences are a reminder that the animal models do not necessarily reflect the human processes in their entirety. Our studies allow us to determine which pathways best reflect the human disease and can be further investigated in the appropriate mouse models.

An obvious limitation is that a “specific transcriptional macrophage signature” cannot be definitively attributed in the context of whole organ sampling, because some of the mRNAs expressed by isolated F4/80<sup>hi</sup> cells may also be expressed either in the same or opposite direction by other resident cells. For example, although Myc expression is downregulated in isolated F4/80<sup>hi</sup> cells, reflecting their maturation status, it is upregulated in whole mouse kidneys. Nevertheless, our study has generated hypotheses that can now be tested in the relevant murine models. In particular, by enhancing or antagonizing specific functions of these cells, it may be possible to identify which of their functions are protective and which are pathogenic. This could lead to new strategies that harness their therapeutic potential.

In summary, our study identified the renal transcriptional features common in human LN and three LN murine models; this strategy will help the scientific community to select the appropriate model to study pathways or pathogenic processes of interest. These common characteristics can further form the basis for new therapeutic strategies. Conversely, characteristics unique to each of the three murine models might be exploited to classify patients for further studies based on their renal molecular profiles. Our study highlights the contribution of renal mononuclear phagocytic cells in both mouse and man, with both phenotypic similarities and differences in gene expression between the glomerular and tubulointerstitial compartments. We can now explore the functional and therapeutic implications of these findings, confirmed in humans, by

further experimentation in our mouse models. This bidirectional flow of information should allow us to discover new therapeutic opportunities, as well as to identify genes that are biomarkers for clinical disease stage or outcome.

## Acknowledgments

We thank the University of Michigan Microarray Core Facility (Cancer Center) for human DNA chip hybridizations and Greg Khitrov for mouse DNA chip hybridizations; Dr. Nicolas Kozakowski (Department of Surgical Pathology, University of Vienna, Vienna, Austria) for providing archival biopsies from LN; Jignesh M. Patel for tool development (TALE); and Stefanie Gaiser (Division of Nephrology, University Hospital) for help with TaqMan real-time PCR. We are grateful to all of the members of the ERCB-Kröner-Fresenius biopsy bank at the time of the study: C.D. Cohen, M. Fischereder, H. Schmid, P.J. Nelson, M. Kretzler, D. Schloendorff, W. Samtleben (Münich); J.D. Sraer, P. Ronco (Paris); M.P. Rastaldi, G. D’Amico (Milan); F. Mampaso (Madrid); P. Doran, H.R. Brady (Dublin); D. Moenks (Goettingen); P. Mertens, J. Floege (Aachen); N. Braun, T. Risler (Tübingen); L. Gesualdo, F.P. Schena (Bari); J. Gerth, G. Wolf (Jena); R. Oberbauer, D. Kerjaschki (Vienna); B. Banas, B.K. Kraemer (Regensburg); H. Peters, H.H. Neumayer (Berlin); K. Ivens, B. Grabensee (Duesseldorf); R.P. Wuehrich (Zurich); and V. Tesar (Prague).

## Disclosures

The authors have no financial conflicts of interest.

## References

- Doria, A., L. Iaccarino, A. Ghirardello, S. Zampieri, S. Arienti, P. Sarzi-Putini, F. Atzeni, A. Piccoli, and S. Todesco. 2006. Long-term prognosis and causes of death in systemic lupus erythematosus. *Am. J. Med.* 119: 700–706.
- Cook, R. J., D. D. Gladman, D. Pericak, and M. B. Urowitz. 2000. Prediction of short term mortality in systemic lupus erythematosus with time dependent measures of disease activity. *J. Rheumatol.* 27: 1892–1895.
- Ward, M. M. 2000. Changes in the incidence of end-stage renal disease due to lupus nephritis, 1982–1995. *Arch. Intern. Med.* 160: 3136–3140.
- Ward, M. M. 2009. Changes in the incidence of endstage renal disease due to lupus nephritis in the United States, 1996–2004. *J. Rheumatol.* 36: 63–67.
- Grande, J. P. 2011. Experimental models of lupus nephritis. *Contrib. Nephrol.* 169: 183–197.
- Davidson, A., and C. Aranow. 2010. Lupus nephritis: lessons from murine models. *Nat Rev Rheumatol* 6: 13–20.
- Henry, T., and C. Mohan. 2005. Systemic lupus erythematosus—recent clues from congenic strains. *Arch. Immunol. Ther. Exp. (Warsz.)* 53: 207–212.
- Lu, Y., R. Rosenfeld, G. J. Nau, and Z. Bar-Joseph. 2010. Cross species expression analysis of innate immune response. *J. Comput. Biol.* 17: 253–268.
- Mestas, J., and C. C. Hughes. 2004. Of mice and not men: differences between mouse and human immunology. *J. Immunol.* 172: 2731–2738.
- Andrews, B. S., R. A. Eisenberg, A. N. Theofilopoulos, S. Izui, C. B. Wilson, P. J. McConahey, E. D. Murphy, J. B. Roths, and F. J. Dixon. 1978. Spontaneous murine lupus-like syndromes. Clinical and immunopathological manifestations in several strains. *J. Exp. Med.* 148: 1198–1215.
- Helyer, B. J., and J. B. Howie. 1963. Renal disease associated with positive lupus erythematosus tests in a cross-bred strain of mice. *Nature* 197: 197.
- Singh, R. R., V. Saxena, S. Zang, L. Li, F. D. Finkelman, D. P. Witte, and C. O. Jacob. 2003. Differential contribution of IL-4 and STAT4 to the development of lupus nephritis. *J. Immunol.* 170: 4818–4825.
- Shen, N., Q. Fu, Y. Deng, X. Qian, J. Zhao, K. M. Kaufman, Y. L. Wu, C. Y. Yu, Y. Tang, J. Y. Chen, et al. 2010. Sex-specific association of X-linked Toll-like receptor 7 (TLR7) with male systemic lupus erythematosus. *Proc. Natl. Acad. Sci. USA* 107: 15838–15843.
- Kahn, P., M. Ramanujam, R. Bethunaickan, W. Huang, H. Tao, M. P. Madaio, S. M. Factor, and A. Davidson. 2008. Prevention of murine antiphospholipid syndrome by BAFF blockade. *Arthritis Rheum.* 58: 2824–2834.
- Ramanujam, M., and A. Davidson. 2008. Targeting of the immune system in systemic lupus erythematosus. *Expert Rev. Mol. Med.* 10: e2.
- Ferenbach, D., and J. Hughes. 2008. Macrophages and dendritic cells: what is the difference? *Kidney Int.* 74: 5–7.
- Bethunaickan, R., C. C. Berthier, M. Ramanujam, R. Sahu, W. Zhang, Y. Sun, E. P. Bottinger, L. Ivashkiv, M. Kretzler, and A. Davidson. 2011. A unique hybrid renal mononuclear phagocyte activation phenotype in murine systemic lupus erythematosus nephritis. *J. Immunol.* 186: 4994–5003.
- Ramanujam, M., R. Bethunaickan, W. Huang, H. Tao, M. P. Madaio, and A. Davidson. 2010. Selective blockade of BAFF for the prevention and treatment of systemic lupus erythematosus nephritis in NZM2410 mice. *Arthritis Rheum.* 62: 1457–1468.
- Schiffer, L., R. Bethunaickan, M. Ramanujam, W. Huang, M. Schiffer, H. Tao, M. P. Madaio, E. P. Bottinger, and A. Davidson. 2008. Activated renal macrophages are markers of disease onset and disease remission in lupus nephritis. *J. Immunol.* 180: 1938–1947.



20. Schiffer, L., J. Sinha, X. Wang, W. Huang, G. von Gersdorff, M. Schiffer, M. P. Madaio, and A. Davidson. 2003. Short term administration of costimulatory blockade and cyclophosphamide induces remission of systemic lupus erythematosus nephritis in NZB/W F1 mice by a mechanism downstream of renal immune complex deposition. *J. Immunol.* 171: 489–497.
21. Schmid, H., A. Boucherot, Y. Yasuda, A. Henger, B. Brunner, F. Eichinger, A. Nitsche, E. Kiss, M. Bleich, H. J. Gröne, et al. European Renal cDNA Bank (ERCB) Consortium. 2006. Modular activation of nuclear factor-kappaB transcriptional programs in human diabetic nephropathy. *Diabetes* 55: 2993–3003.
22. Cohen, C. D., K. Frach, D. Schlöndorff, and M. Kretzler. 2002. Quantitative gene expression analysis in renal biopsies: a novel protocol for a high-throughput multicenter application. *Kidney Int.* 61: 133–140.
23. Lindenmeyer, M. T., M. Kretzler, A. Boucherot, S. Berra, Y. Yasuda, A. Henger, F. Eichinger, S. Gaiser, H. Schmid, M. P. Rastaldi, et al. 2007. Interstitial vascular rarefaction and reduced VEGF-A expression in human diabetic nephropathy. *J. Am. Soc. Nephrol.* 18: 1765–1776.
24. Berthier, C. C., H. Zhang, M. Schin, A. Henger, R. G. Nelson, B. Yee, A. Boucherot, M. A. Neusser, C. D. Cohen, C. Carter-Su, et al. 2009. Enhanced expression of Janus kinase-signal transducer and activator of transcription pathway members in human diabetic nephropathy. *Diabetes* 58: 469–477.
25. Johnson, W. E., C. Li, and A. Rabinovic. 2007. Adjusting batch effects in microarray expression data using empirical Bayes methods. *Biostatistics* 8: 118–127.
26. Vandesompele, J., K. De Preter, F. Pattyn, B. Poppe, N. Van Roy, A. De Paepe, and F. Speleman. 2002. Accurate normalization of real-time quantitative RT-PCR data by geometric averaging of multiple internal control genes. *Genome Biol.* 3: H0034.
27. Abruzzo, L. V., L. L. Barron, K. Anderson, R. J. Newman, W. G. Wierda, S. O'Brien, A. Ferrajoli, M. Luthra, S. Talwalkar, R. Luthra, et al. 2007. Identification and validation of biomarkers of IgV(H) mutation status in chronic lymphocytic leukemia using microfluidics quantitative real-time polymerase chain reaction technology. *J. Mol. Diagn.* 9: 546–555.
28. Tian, Y., and J. Patel. 2008. TALE: A Tool for Approximate Large Graph Matching. *ICDE, IEEE 24th International Conference on Data Engineering.* 963–972.
29. Cline, M. S., M. Smoot, E. Cerami, A. Kuchinsky, N. Landys, C. Workman, R. Christmas, I. Avila-Campilo, M. Creech, B. Gross, et al. 2007. Integration of biological networks and gene expression data using Cytoscape. *Nat. Protoc.* 2: 2366–2382.
30. Segerer, S., F. Heller, M. T. Lindenmeyer, H. Schmid, C. D. Cohen, D. Draganovici, J. Mandelbaum, P. J. Nelson, H. J. Gröne, E. F. Gröne, et al. 2008. Compartment specific expression of dendritic cell markers in human glomerulonephritis. *Kidney Int.* 74: 37–46.
31. Saeed, A. I., N. K. Bhagabati, J. C. Braisted, W. Liang, V. Sharov, E. A. Howe, J. Li, M. Thiagarajan, J. A. White, and J. Quackenbush. 2006. TM4 microarray software suite. *Methods Enzymol.* 411: 134–193.
32. Saeed, A. I., V. Sharov, J. White, J. Li, W. Liang, N. Bhagabati, J. Braisted, M. Klapa, T. Currier, M. Thiagarajan, et al. 2003. TM4: a free, open-source system for microarray data management and analysis. *Biotechniques* 34: 374–378.
33. Park, M. H., V. D'Agati, G. B. Appel, and C. L. Pirani. 1986. Tubulointerstitial disease in lupus nephritis: relationship to immune deposits, interstitial inflammation, glomerular changes, renal function, and prognosis. *Nephron* 44: 309–319.
34. Fujii, K., and Y. Kobayashi. 1988. Quantitative analysis of interstitial alterations in lupus nephritis. *Virchows Arch. A Pathol. Anat. Histopathol.* 414: 45–52.
35. Hill, G. S., M. Delahousse, D. Nochy, E. Thervet, F. Vrtovnik, P. Rémy, D. Glotz, and J. Bariety. 2002. Outcome of relapse in lupus nephritis: roles of reversal of renal fibrosis and response of inflammation to therapy. *Kidney Int.* 61: 2176–2186.
36. Hsieh, C., A. Chang, D. Brandt, R. Guttikonda, T. O. Utset, and M. R. Clark. 2011. Predicting outcomes of lupus nephritis with tubulointerstitial inflammation and scarring. *Arthritis Care Res (Hoboken)* 63: 865–874.
37. Thacker, S. G., C. C. Berthier, D. Mattinzoli, M. P. Rastaldi, M. Kretzler, and M. J. Kaplan. 2010. The detrimental effects of IFN- $\alpha$  on vasculogenesis in lupus are mediated by repression of IL-1 pathways: potential role in atherogenesis and renal vascular rarefaction. *J. Immunol.* 185: 4457–4469.
38. Duffield, J. S. 2010. Macrophages and immunologic inflammation of the kidney. *Semin. Nephrol.* 30: 234–254.
39. Duffield, J. S. 2011. Macrophages in kidney repair and regeneration. *J. Am. Soc. Nephrol.* 22: 199–201.
40. Lee, S., S. Huen, H. Nishio, S. Nishio, H. K. Lee, B. S. Choi, C. Ruhrberg, and L. G. Cantley. 2011. Distinct macrophage phenotypes contribute to kidney injury and repair. *J. Am. Soc. Nephrol.* 22: 317–326.
41. Wang, A., A. M. Fairhurst, K. Tus, S. Subramanian, Y. Liu, F. Lin, P. Igarashi, X. J. Zhou, F. Batteux, D. Wong, et al. 2009. CXCR4/CXCL12 hyperexpression plays a pivotal role in the pathogenesis of lupus. *J. Immunol.* 182: 4448–4458.
42. Wang, A., P. Guilpain, B. F. Chong, S. Chouzenoux, L. Guillemin, Y. Du, X. J. Zhou, F. Lin, A. M. Fairhurst, C. Boudreaux, et al. 2010. Dysregulated expression of CXCR4/CXCL12 in subsets of patients with systemic lupus erythematosus. *Arthritis Rheum.* 62: 3436–3446.
43. Chang, A., S. G. Henderson, D. Brandt, N. Liu, R. Guttikonda, C. Hsieh, N. Kaverina, T. O. Utset, S. M. Meehan, R. J. Quigg, et al. 2011. In situ B cell-mediated immune responses and tubulointerstitial inflammation in human lupus nephritis. *J. Immunol.* 186: 1849–1860.
44. Peterson, K. S., J. F. Huang, J. Zhu, V. D'Agati, X. Liu, N. Miller, M. G. Erlander, M. R. Jackson, and R. J. Winchester. 2004. Characterization of heterogeneity in the molecular pathogenesis of lupus nephritis from transcriptional profiles of laser-captured glomeruli. *J. Clin. Invest.* 113: 1722–1733.
45. Soos, T. J., T. N. Sims, L. Barisoni, K. Lin, D. R. Littman, M. L. Dustin, and P. J. Nelson. 2006. CX3CR1+ interstitial dendritic cells form a contiguous network throughout the entire kidney. *Kidney Int.* 70: 591–596.
46. Krüger, T., D. Benke, F. Eitner, A. Lang, M. Wirtz, E. E. Hamilton-Williams, D. Engel, B. Giese, G. Müller-Newen, J. Floege, and C. Kurtz. 2004. Identification and functional characterization of dendritic cells in the healthy murine kidney and in experimental glomerulonephritis. *J. Am. Soc. Nephrol.* 15: 613–621.
47. Suzuki, T., H. Kono, N. Hirose, M. Okada, T. Yamamoto, K. Yamamoto, and Z. Honda. 2000. Differential involvement of Src family kinases in Fc gamma receptor-mediated phagocytosis. *J. Immunol.* 165: 473–482.
48. Lindenmeyer, M., E. Noessner, P. J. Nelson, and S. Segerer. 2011. Dendritic cells in experimental renal inflammation—Part I. *Nephron Exp. Nephrol.* 119: e83–e90.
49. Noessner, E., M. Lindenmeyer, P. J. Nelson, and S. Segerer. 2011. Dendritic cells in human renal inflammation—Part II. *Nephron Exp. Nephrol.* 119: e91–e98.
50. Xiao, W., H. Hong, Y. Kawakami, C. A. Lowell, and T. Kawakami. 2008. Regulation of myeloproliferation and M2 macrophage programming in mice by Lyn/Hck, SHIP, and Stat5. *J. Clin. Invest.* 118: 924–934.
51. Totani, L., A. Piccoli, S. Manarini, L. Federico, R. Pecce, N. Martelli, C. Cerletti, P. Piccardoni, C. A. Lowell, S. S. Smyth, et al. 2006. Src-family kinases mediate an outside-in signal necessary for beta2 integrins to achieve full activation and sustain firm adhesion of polymorphonuclear leucocytes tethered on E-selectin. *Biochem. J.* 396: 89–98.
52. Fitzer-Attas, C. J., M. Lowry, M. T. Crowley, A. J. Finn, F. Meng, A. L. DeFranco, and C. A. Lowell. 2000. Fc gamma receptor-mediated phagocytosis in macrophages lacking the Src family tyrosine kinases Hck, Fgr, and Lyn. *J. Exp. Med.* 191: 669–682.
53. Chong, B. F., and C. Mohan. 2009. Targeting the CXCR4/CXCL12 axis in systemic lupus erythematosus. *Expert Opin. Ther. Targets* 13: 1147–1153.
54. Amanullah, A., D. A. Liebermann, and B. Hoffman. 2002. Deregulated c-Myc prematurely recruits both Type I and II CD95/Fas apoptotic pathways associated with terminal myeloid differentiation. *Oncogene* 21: 1600–1610.
55. Van Dang, C., and S. B. McMahon. 2010. Emerging Concepts in the Analysis of Transcriptional Targets of the MYC Oncoprotein: Are the Targets Targetable? *Genes Cancer* 1: 560–567.
56. Rigamonti, E., G. Chinetti-Gbaguidi, and B. Staels. 2008. Regulation of macrophage functions by PPAR-alpha, PPAR-gamma, and LXRs in mice and men. *Arterioscler. Thromb. Vasc. Biol.* 28: 1050–1059.
57. Chawla, A., Y. Barak, L. Nagy, D. Liao, P. Tontonoz, and R. M. Evans. 2001. PPAR-gamma dependent and independent effects on macrophage-gene expression in lipid metabolism and inflammation. *Nat. Med.* 7: 48–52.
58. Majai, G., Z. Sarang, K. Csomós, G. Zahuczky, and L. Fésüs. 2007. PPARgamma-dependent regulation of human macrophages in phagocytosis of apoptotic cells. *Eur. J. Immunol.* 37: 1343–1354.
59. Aprahamian, T., R. G. Bonegio, C. Richez, K. Yasuda, L. K. Chiang, K. Sato, K. Walsh, and I. R. Rifkin. 2009. The peroxisome proliferator-activated receptor gamma agonist rosiglitazone ameliorates murine lupus by induction of adiponectin. *J. Immunol.* 182: 340–346.
60. Zhao, W., S. G. Thacker, J. B. Hodgins, H. Zhang, J. H. Wang, J. L. Park, A. Randolph, E. C. Somers, S. Pennathur, M. Kretzler, et al. 2009. The peroxisome proliferator-activated receptor gamma agonist pioglitazone improves cardiometabolic risk and renal inflammation in murine lupus. *J. Immunol.* 183: 2729–2740.
61. Pahl, M. V., N. D. Vaziri, J. Yuan, and S. G. Adler. 2010. Upregulation of monocyte/macrophage HGFIN (Gpmb/Osteoactivin) expression in end-stage renal disease. *Clin. J. Am. Soc. Nephrol.* 5: 56–61.
62. Psarras, S., M. Mavroidis, D. Sanoudou, C. H. Davos, G. Xanthou, A. E. Varela, V. Panoutsakopoulou, and Y. Capetanaki. 2011. Regulation of adverse remodeling by osteopontin in a genetic heart failure model. *Eur. Heart J.* 10.1093/eurheartj/ehr119.